

# Optical radiation background from $^{40}\text{K}$ decays in undersea neutrino telescopes

F. Massa<sup>a</sup>

Istituto Nazionale di Fisica Nucleare, Sezione di Roma, 00185 Roma, Italy

Received: 29 August 2001 / Revised version: 25 October 2001 /  
Published online: 14 December 2001 – © Springer-Verlag / Società Italiana di Fisica 2001

**Abstract.** The photon flux produced by light sources uniformly distributed in an infinite homogeneous medium is calculated on the basis of a known property of light propagation, taking into account the contribution of both absorption and scattering processes. The results are applied to the issue of the decays of  $^{40}\text{K}$  content in sea salt and then to the rates detected by photomultipliers deployed in the deep sea. Numerical calculations are in agreement with the recent measurements performed in the Mediterranean Sea by the ANTARES and NEMO Collaborations.

## 1 Introduction

The search for high energy astrophysical neutrino sources requires very large experimental apparatus (on the scale of a cubic kilometer) and maximum reduction of the cosmic ray background in order to detect the faint signals from distant cosmic objects. The need for a large detector volume has led to various projects: in the deep sea (ANTARES, NEMO, NESTOR), in the Antarctic ice (AMANDA) and in freshwater (BAIKAL).

Water (or ice) acts as an active medium in three ways: it is the target on which the neutrinos produce charged particles, it generates Čerenkov light by interacting with these charged particles and it is the propagation medium of the light to the detector. The direction of an incoming neutrino is deduced from that of the muons produced in the interactions with the water or ice. The muon trajectory is, in turn, reconstructed from the arrival time of the Čerenkov light at the photomultipliers (PMTs) of the apparatus.

Deep sea experiments experience three different sources of background:

1. the residual down going cosmic ray still present even at the deep location of the apparatus (common in ice or fresh water experiments);
2. light from bioluminescent organisms;
3. light due to the decays of an unstable potassium isotope ( $^{40}\text{K}$ ) contained in sea salt.

A large fraction of the primary and secondary electrons produced in  $^{40}\text{K}$  decays are above the threshold for Čerenkov light emission. The absorption length of clean water is large in the visible spectrum ( $> 50\text{ m}$ ). Hence a

large volume of seawater contributes to the photon flux, which in the calculations below turns out to be of the order of  $500\text{ cm}^{-2}\text{ s}^{-1}$ , in spite of the small amount of  $^{40}\text{K}$  contained in a unit volume. Moreover in undersea neutrino telescopes PMTs must be sensitive to a single photoelectron in order to achieve good muon track reconstruction. For all these reasons it is clear that the light produced in  $^{40}\text{K}$  decays is the main background, even if in some cases, depending on the site, light from bioluminescence can also be significant.

In this paper we calculate the rate of photons of different wavelengths coming from  $^{40}\text{K}$  decays and crossing a  $\text{cm}^2$  surface at a point in the sea. On this basis we are then able to calculate the rate of a PMT deployed in the deep sea. The final result, obtained by numerical integration, depends on the light production mechanism, on the properties of seawater light transport and on the detector employed. In particular the photon spectrum is specific to the process under consideration ( $^{40}\text{K}$  decay) and the detector characteristics (geometry, acceptance, quantum efficiency etc.) are also specific to the apparatus. However, apart from this, the procedure followed (Sect. 2.1) is fairly general and is based on a known property of light transport in an infinite homogeneous medium. In calculating this flux the relevance of both scattering and absorption processes experienced by photons is pointed out. A rule of internal consistency is also found for Monte Carlo calculations, where scattering processes must be taken into account. An alternative procedure, based on an iterative process, is developed in Sect. 2.2. The results are then applied to the calculation of the flux induced by  $^{40}\text{K}$  decays in seawater. The number of photons produced in such decays is calculated in Sect. 3. In Sect. 4 the photon flux at different wavelengths and, from this, the PMT rate expected in the deep sea is calculated and compared with

<sup>a</sup> e-mail: fabrizio.massa@roma1.infn.it

the experimental results. In Sect. 5 the contributions of direct and scattered light are calculated.

## 2 Photon flux from a light source uniformly distributed in an infinite homogeneous medium

In the following we consider a homogeneous medium (for example the sea) having an infinite extension with respect to its own absorption length and containing a uniformly distributed light source (for example  $^{40}\text{K}$ ), which emits isotropic light. We assume that during the entire passage of the light through the medium its wavelength remains unchanged and no buildup of further photons occurs. Regarding light coming from  $^{40}\text{K}$  decays in seawater, this means considering scattering by water molecules only and ignoring fluorescence effects, since in the region of interest of the wavelengths (300 ÷ 600 nm) Raman scattering is negligible compared to the absorption process [1]. This allows us to deal, in the following, with the number of photons as well as their energy.

The interaction of these photons with the medium is calculated in terms of absorption ( $L_{\text{ab}}$ ) and scattering ( $L_{\text{sc}}$ ) lengths and their dependence on the wavelength  $\lambda$ . Let us initially consider monochromatic photons, so that we can omit the explicit  $\lambda$  dependence in the parameters. The following equation is valid:

$$\frac{1}{L_{\text{at}}} = \frac{1}{L_{\text{ab}}} + \frac{1}{L_{\text{sc}}}. \quad (1)$$

The quantity  $e^{-r/L_{\text{at}}}$  measures the residual fraction of the photons in a collimated beam after they have crossed a length  $r$  of the medium, while the fraction  $e^{-r/L_{\text{ab}}}$  is lost, since it is outside the sensitivity range of the detector.

We calculate the photon flux at a point in the medium in two ways: in Sect. 2.1 we proceed on the basis of a known general physics result. In Sect. 2.2 we calculate using iteration the intensity of light scattered in a  $\text{cm}^3$  of the medium and then, from this, the expected photon flux.

### 2.1 Calculation on general grounds

A known result of radiological physics states that in an infinite homogeneous medium uniformly filled by a radiation source, the rate per unit volume of the radiation absorption must be equal to the rate of production [2]. This is precisely the case regarding the sea and  $^{40}\text{K}$  decay, where the dimension of the sea is much larger than the absorption length of the radiation. The result can be understood in the following terms. Let us put a radiation source of intensity  $I_0$  (number of photons  $\text{s}^{-1}$ ) at a point  $P_0$  of the medium. Let us also call  $I(P)$  the intensity of the radiation propagated from this source up to the point  $P$ , and  $I_{\text{sc}}(P)$  and  $I_{\text{ab}}(P)$ , respectively, the intensity scattered away and absorbed by the medium at  $P$ . If this medium is infinitely large compared to the absorption length of the radiation,

that is if no photons flow out of the boundary surface of the medium, the conservation of energy requires that the intensity  $I_0$  is absorbed by the medium surrounding  $P_0$ . So we have

$$\sum I_{\text{ab}}(P) = I_0, \quad (2)$$

where the sum can be extended over the entire medium, assuming there is zero contribution from the points where no radiation arrives.

A scenario reciprocal to the previous one can be built on the basis of the Helmholtz reciprocity theorem for optics [3]. This states that if a source of intensity  $I_0$  located at point  $P_0$  produces intensity  $I$  at point  $P$ , the same source located at  $P$  produces intensity  $I$  at  $P_0$ . Moreover in the case of a homogeneous medium the fraction of the radiation intensity  $I$  absorbed at a point does not depend on the position of the point in the medium, so that the same intensity  $I_{\text{ab}}$  is absorbed at  $P_0$  when the source is at  $P$ . Now, if we build a reciprocal scenario to that of (2), simply distributing sources of the same intensity  $I_0$  throughout the medium, we obtain the situation we want to study. Point  $P$  contributes the amount  $I_{\text{ab}}(P)$ , which may be zero, to the intensity absorbed in  $P_0$ , which becomes, from (2),

$$I_{\text{ab}}(P_0) = \sum I_{\text{ab}}(P) = I_0. \quad (3)$$

From this equation it is easy to derive the photon flux at a point in the medium in the case of a continuous distribution of sources of the same intensity  $I_0$  (number of photons  $\text{cm}^{-3} \text{s}^{-1}$ ) throughout the entire medium. The number of photons crossing a single face of an elementary plane surface  $dS$  in time  $dt$  can be calculated by integrating over half the total solid angle ( $\Omega_{\text{tot}}/2$ ) the number of photons per steradian,  $\text{cm}^2$  and second:

$$dN = dS dt \int_{\Omega_{\text{tot}}/2} d\Omega \frac{dN}{d\Omega dS_{\perp} dt} \cos \theta,$$

where  $dS_{\perp}$  is the projection of the area  $dS$  on the direction perpendicular to  $d\Omega$  and  $\theta$  is the angle between the photon direction and the normal to  $dS$ . Since, in our case, the photon flux per steradian is isotropic, we have

$$\begin{aligned} \frac{dN}{dS dt} &= \frac{dN}{d\Omega dS_{\perp} dt} \int_{\Omega_{\text{tot}}/2} d\Omega \cos \theta \\ &= \pi \frac{dN}{d\Omega dS_{\perp} dt}. \end{aligned} \quad (4)$$

Now we calculate the rate of photon absorption per  $\text{cm}^3$  and second ( $dN_{\text{ab}}/dV dt$ ) from the photon flux ( $dN/dS dt$ ). Considering an element of volume  $dV$  limited by a pair of parallel plane surface  $dS$  separated by a small distance  $dx$ , so that we can neglect the flux across the lateral surface, we have

$$dN_{\text{ab}} = 2dS dt \int_{\Omega_{\text{tot}}/2} d\Omega \frac{dN}{d\Omega dS_{\perp} dt} \cos \theta \frac{dx/\cos \theta}{L_{\text{ab}}}, \quad (5)$$

where  $dx/\cos\theta$  is the length crossed by the photons in the volume  $dV$ , so that  $(dx/\cos\theta)/L_{\text{ab}}$  is the fraction of the photons absorbed in  $dV$ . The factor two is due to the fact that photons enter the volume from both faces. From (5), since  $dV = dSdx$ , we have

$$\begin{aligned}\frac{dN_{\text{ab}}}{dVdt} &= 2 \frac{dN}{d\Omega dS_{\perp} dt} \frac{1}{L_{\text{ab}}} \int_{\Omega_{\text{tot}}/2} d\Omega \\ &= 4\pi \frac{dN}{d\Omega dS_{\perp} dt} \frac{1}{L_{\text{ab}}}.\end{aligned}$$

Using (4) we obtain

$$\frac{dN}{dSdt} = \frac{dN_{\text{ab}}}{dVdt} \frac{L_{\text{ab}}}{4}. \quad (6)$$

From (3), which states

$$\frac{dN_{\text{ab}}}{dVdt} = I_0,$$

we have

$$\frac{dN}{dSdt} = I_0 \frac{L_{\text{ab}}}{4}. \quad (7)$$

Following the same procedure used in (5), we can calculate the rate of photons scattered per  $\text{cm}^3$  and second simply by substituting  $L_{\text{ab}}$  with  $L_{\text{sc}}$ , so that we have, from (6) and (7),

$$I_{\text{sc}} = \frac{dN_{\text{sc}}}{dVdt} = \frac{dN}{dSdt} \frac{4}{L_{\text{sc}}} = I_0 \frac{L_{\text{ab}}}{L_{\text{sc}}}. \quad (8)$$

To calculate the total rate  $I$  of the photons entering a unit volume, we can sum the rates of the photons absorbed and scattered in that volume:

$$I = I_{\text{ab}} + I_{\text{sc}}.$$

From (3), (8) and (1) we have

$$\begin{aligned}I &= I_0 + I_0 \frac{L_{\text{ab}}}{L_{\text{sc}}} \\ &= I_0 L_{\text{ab}} \left( \frac{1}{L_{\text{ab}}} + \frac{1}{L_{\text{sc}}} \right) = I_0 \frac{L_{\text{ab}}}{L_{\text{at}}}. \quad (9)\end{aligned}$$

Because the rate of radiation absorption is equal to the rate of production, this latter result also gives the intensity of the light *coming out* of a unit volume. This intensity receives the contributions of both the light *produced* in the unit volume and of the light produced in the surrounding medium and scattered in that volume.

Considering now the wavelength dependence of the photon production rate  $I_0$  (now: number of photons  $\text{cm}^{-3} \text{s}^{-1} \text{nm}^{-1}$ ) and of the absorption and scattering lengths, the flux of photons at the wavelength  $\lambda$  is

$$\Phi(\lambda) = I_0(\lambda) \frac{L_{\text{ab}}(\lambda)}{4}. \quad (10)$$

We suggest that, whenever the Monte Carlo method is employed to calculate the photon flux, (3) should be used

as an internal consistency check. If  $\Phi(\lambda)$  is the computed photon flux, using (6) the quantity

$$4 \int_{\lambda_1}^{\lambda_2} d\lambda \frac{\Phi(\lambda)}{L_{\text{ab}}(\lambda)}$$

integrated over a given volume should be equal to the photon rate generated by the Monte Carlo in that volume. We also point out that ignoring scattering effects one underestimates the photon flux by a factor  $L_{\text{ab}}/L_{\text{at}}$  for each wavelength (see Sect. 5). In Sect. 3 we calculate the value of  $I_0$  in the case of  $^{40}\text{K}$  decays in the sea.

## 2.2 Iterative calculation

In this section, in order to calculate the photon flux, we start by distinguishing between the light *produced* or *generated* in a volume of the medium and the light *coming out of* or *emitted by* that volume, as was done at the end of Sec.2.1. In fact the total light of intensity  $I$  (number of photons  $\text{cm}^{-3} \text{s}^{-1}$ ; again initially we consider monochromatic light) emitted by a unit volume is composed of the light, of intensity  $I_0$ , produced by the sources contained in that volume, and the light, of intensity  $I_{\text{sc}}$ , produced in the surrounding medium and scattered in that volume.

We can write

$$I = I_0 + I_{\text{sc}}. \quad (11)$$

To calculate the rate of photons emitted by an element of volume  $d\tau$  and scattered in a second element of volume  $dV$ , we proceed in an iterative way. First we consider the light generated in  $d\tau$  to be the only light emitted by  $d\tau$ , ignoring the light generated in the surrounding medium and scattered in  $d\tau$ . In this approximation we calculate the amount of light scattered in  $dV$  integrating over the whole space  $\tau$ . This value, scaled to the volume  $d\tau$  and summed to the intensity of light generated in this volume  $d\tau$ , gives a second approximation for the total light emitted by  $d\tau$ , which is used as input for a second step and so on. Obviously the possibility for the two volumes  $d\tau$  and  $dV$  to exchange roles is based on the validity of the reciprocity theorem of optics, as explained in the previous section.

So, as a first approximation, we set

$$(I)^0 = I_0, \quad (I_{\text{sc}})^0 = 0$$

and we consider  $I_0 d\tau$  to be the total light emitted by the volume  $d\tau$ . Let us consider the volume  $dV$ , located at a distance  $r$  from  $d\tau$ , to be limited by a pair of parallel plane surfaces  $dS$ , separated by a small distance  $dx$ , as in the previous section. In the present approximation the rate of the light scattered away in the volume  $dV$  is

$$\left( \frac{dN_{\text{sc}}}{dt} \right)^0 = I_0 \frac{\cos\theta dS}{4\pi r^2} \frac{dx/\cos\theta}{L_{\text{sc}}} e^{-r/L_{\text{at}}} d\tau, \quad (12)$$

where  $(\cos\theta dS)/(4\pi r^2)$  is the fraction of solid angle defined by the surface  $dS$  with respect to  $d\tau$ ,  $\theta$  the angle

between the direction of the photons coming from  $d\tau$  and the perpendicular to  $dS$  and  $(dx/\cos\theta)/L_{sc}$  the fraction of these photons scattered away while crossing  $dV$ .

From (12) we have

$$\left(\frac{dN_{sc}}{dVdt}\right)^0 = \frac{I_0}{4\pi r^2 L_{sc}} e^{-r/L_{at}} d\tau.$$

Integrating over the whole space  $\tau$  we have

$$\left(\frac{dN_{sc}}{dVdt}\right)^0 = I_0 \frac{L_{at}}{L_{sc}}.$$

Now, as a second approximation for the light scattered in  $d\tau$ , we put

$$(I_{sc})^1 = \left(\frac{dN_{sc}}{d\tau dt}\right)^0 = I_0 \frac{L_{at}}{L_{sc}} \quad (13)$$

and we obtain, in the same approximation, the light emitted by  $d\tau$

$$\begin{aligned} (I)^1 &= I_0 + (I_{sc})^1 \\ &= I_0 \left(1 + \frac{L_{at}}{L_{sc}}\right). \end{aligned}$$

As a second step we replace  $I_0$  in (12) by  $(I)^1$  and so on.

Proceeding in this way we arrive at

$$\begin{aligned} I_{sc} &= I_0 \left( \frac{L_{at}}{L_{sc}} + \left(\frac{L_{at}}{L_{sc}}\right)^2 + \dots + \left(\frac{L_{at}}{L_{sc}}\right)^n + \dots \right) \\ &= I_0 \frac{L_{at}}{L_{sc}} \left( 1 + \frac{L_{at}}{L_{sc}} + \dots + \left(\frac{L_{at}}{L_{sc}}\right)^{n-1} + \dots \right) \end{aligned}$$

and

$$I = I_0 \left( 1 + \frac{L_{at}}{L_{sc}} + \dots + \left(\frac{L_{at}}{L_{sc}}\right)^n + \dots \right).$$

Since  $L_{at} < L_{sc}$  (see (1)) the sums at the second members of both these equations converge to the value

$$\frac{1}{1 - \frac{L_{at}}{L_{sc}}},$$

so that we have

$$\begin{aligned} I_{sc} &= I_0 \frac{L_{at}}{L_{sc}} \frac{1}{1 - \frac{L_{at}}{L_{sc}}} = I_0 \frac{L_{at}}{L_{sc}} \frac{1}{L_{ab}} \\ &= I_0 \frac{L_{ab}}{L_{sc}} = (8) \end{aligned} \quad (14)$$

and

$$I = \frac{I_0}{1 - \frac{L_{at}}{L_{sc}}} = I_0 \frac{L_{ab}}{L_{at}} = (9). \quad (15)$$

Obviously from (14) and (15) we have

$$\begin{aligned} I - I_{sc} &= I_0 \left( \frac{L_{ab}}{L_{at}} - \frac{L_{ab}}{L_{sc}} \right) \\ &= I_0 L_{ab} \left( \frac{1}{L_{at}} - \frac{1}{L_{sc}} \right) = I_0, \end{aligned}$$

as expected from (11).

To calculate the rate of photons *emitted* by  $d\tau$  and absorbed by  $dV$  we can write, in analogy to (12),

$$\frac{dN_{ab}}{dt} = I \frac{\cos\theta dS}{4\pi r^2} \frac{dx/\cos\theta}{L_{ab}} e^{-r/L_{at}} d\tau, \quad (16)$$

because  $I$ , the total light intensity emitted per unit volume, given by (15), contains the scattering contribution. Integrating over the whole space  $\tau$  we obtain, in analogy to (13),

$$\begin{aligned} I_{ab} &= I \frac{L_{at}}{L_{ab}} = I_0 \frac{L_{ab}}{L_{at}} \frac{L_{at}}{L_{ab}} \\ &= I_0 = (3). \end{aligned}$$

The rate of photons *emitted* by  $d\tau$  and crossing the element of surface  $dS$  is

$$\frac{dN}{dt} = I \frac{\cos\theta dS}{4\pi r^2} e^{-r/L_{at}} d\tau. \quad (17)$$

Substituting the value of  $I$  from (15) in this equation and integrating over the whole volume  $\tau$  we have

$$\frac{dN}{dSdt} = I_0 \frac{L_{ab}}{4} = (7).$$

### 3 Light intensity from $^{40}\text{K}$ decays in seawater

Potassium is one of the major constituents of the salinity of seawater. It has been found that, except in regions of high dilution or near the shore, the ratio between the major ionic components of sea salt is constant regardless of the value of the salinity Sl (grams of melt salt per kg of water or ‰) [4].

Natural potassium contains the radioactive  $^{40}\text{K}$  isotope with a weight ratio of [5]

$$w_1 = .0117\%.$$

Thus the content  $R$  of  $^{40}\text{K}$  in seawater can be stated as depending on the site salinity Sl

$$R = w_1 w_2 w_3 \frac{\text{Sl}}{\text{Sl}_0},$$

where  $w_2$  and  $w_3$  are, respectively, the weight ratio of potassium to chlorine and of chlorine to a reference salinity  $\text{Sl}_0$ . Numerically, for the Mediterranean Sea, we have [6]

$$w_2 = .02008 \text{ g kg}^{-1}$$

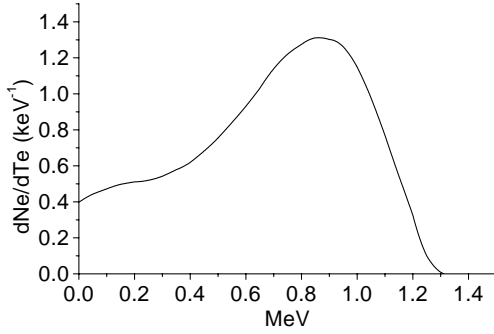


**Fig. 1.**  $\beta^-$  spectrum from  $^{40}\text{K}$  decay (branching ratio: 89.3%)

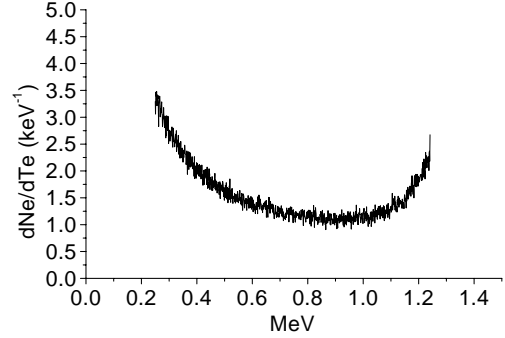


**Fig. 2.** Monte Carlo calculation of the electron spectrum from the Compton scattering of a  $\gamma$  of 1.461 MeV. The  $\gamma$  follows the electron capture in  $^{40}\text{K}$  decay (branching ratio: 10.7%)

and

$$w_3 = 18.98 \text{ g kg}^{-1}$$

at salinity

$$\text{Sl}_0 = 34.5 \text{ ‰}$$

so that

$$R = 4.46 \times 10^{-5} \frac{\text{Sl}}{\text{Sl}_0} \text{ g kg}^{-1}.$$

For instance at the KM3 NEMO site (see Sect. 4), where  $\text{Sl} = 38.7 \text{ ‰}$  [7], we have

$$R = 5 \times 10^{-5} \text{ g kg}^{-1}.$$

The activity Act of  $^{40}\text{K}$  can be calculated on the basis of the salinity Sl of the site:

$$\text{Act} = \frac{\ln 2}{T_{1/2}} \frac{N_A}{A} \rho R,$$

where  $N_A$  is the Avogadro number,  $A$  the potassium atomic mass number,

$$T_{1/2} = 1.277 \times 10^9 \text{ years}$$

the  $^{40}\text{K}$  half-time and  $\rho$  the water density. At a depth of 3000 m in the KM3 NEMO site, where [8]

$$\rho = 1.03 \text{ g cm}^{-3},$$

we have

$$\text{Act} = 1.36 \times 10^{-2} \text{ Bq cm}^{-3}.$$

$^{40}\text{K}$  decays in two main modes releasing electrons [5]:

1.  $\beta^-$ , with a branching ratio of 89.3%. The electron spectrum of this mode is shown in Fig. 1. It shows a kinetic energy endpoint at 1.311 MeV.
2. Electron capture, with a branching ratio of 10.7%, followed by a  $\gamma$  ray of 1.461 MeV. The  $\gamma$  in turn interacts with seawater and releases electrons by Compton scattering. The spectrum of these electrons, resulting from a Monte Carlo calculation, is reported in Fig. 2 for electron kinetic energies greater than the Čerenkov threshold.

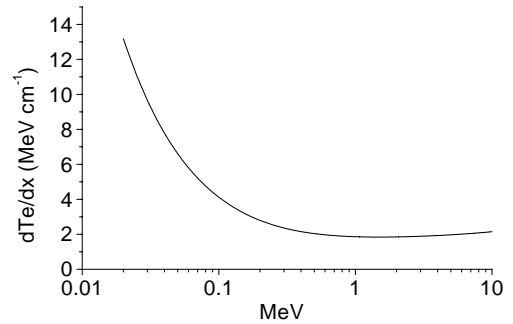


**Fig. 3.** Energy loss of electrons in water

These electrons slow down and lose energy when they interact with seawater. Čerenkov light is emitted in water by electrons with kinetic energy greater than  $T_{\text{thr}} = 250 \text{ keV}$  (the refraction index  $n$  of seawater is 1.35 at salinity 38.7‰ and temperature 15°C [4]).

The number of photons produced per unitary wavelength interval by electrons in the unitary interval of kinetic energy ( $dN/(dT_e d\lambda)$ , number of photons  $\text{keV}^{-1} \text{ nm}^{-1}$ ) can be calculated on the basis of

1. the electron spectrum  $dN_e/dT_e$  resulting from the weighted sum of the spectra of Figs. 1 and 2;
2. the electron energy losses in water  $dT/dx$  ([9], see Fig. 3);
3. the number of Čerenkov photons produced per unitary electron path length and photon wavelength interval,

$$\frac{dN_{\check{\text{C}}\text{er}}}{dx d\lambda} = \left(1 - \frac{1}{\beta^2 n^2}\right) \frac{2\pi\alpha}{\lambda^2},$$

where  $\alpha = 1/137$ .

Thus

$$\frac{dN}{dT_e d\lambda} = \frac{dN_e}{dT_e} \int_{T_{\text{thr}}}^{T_e} dT \frac{1}{\left(\frac{dT}{dx}\right)} \frac{dN_{\check{\text{C}}\text{er}}}{dx d\lambda}. \quad (18)$$

The numerical integration of (18) in the wavelength interval  $\lambda_1 = 300 \text{ nm} - \lambda_2 = 600 \text{ nm}$ :

$$\frac{dN}{dT_e} = \frac{dN_e}{dT_e} \int_{T_{\text{thr}}}^{T_e} dT \frac{1}{\frac{dT}{dx}} \int_{\lambda_1}^{\lambda_2} d\lambda \frac{dN_{\check{\text{C}}\text{er}}}{dx d\lambda}$$

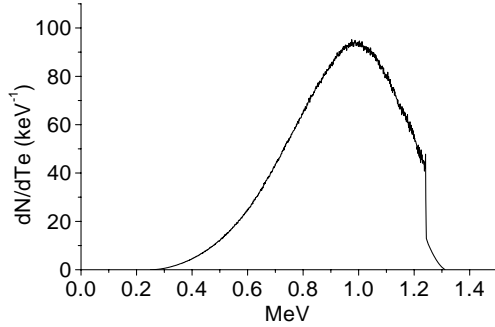


**Fig. 4.** Number of photons versus electron kinetic energy

is shown in Fig. 4. So, integrating over the available electron energies, we have

$$N_0 = 46.2$$

photons per  $^{40}\text{K}$  decay in the interval  $300 \text{ nm} < \lambda < 600 \text{ nm}$ . Alternatively, integrating first (18) over the electron energies, we have

$$N = \ell \left( \frac{1}{\lambda_1} - \frac{1}{\lambda_2} \right), \quad (19)$$

where  $\ell$  is a length independent of the wavelength. From this equation and the  $N_0$  value we have

$$\ell = 2.77 \times 10^{-3} \text{ cm.}$$

Equation (19) together with the  $\ell$  value allows us to compute the number of photons produced in  $^{40}\text{K}$  decays in any given wavelength interval. The number of photons produced per unit of volume, time and wavelength can be written

$$I_0(\lambda) = \frac{\text{Act}\ell}{\lambda^2}. \quad (20)$$

Substituting  $I_0$  from this equation in (10), we obtain the photon flux at wavelength  $\lambda$ :

$$\Phi(\lambda) = \frac{\text{Act}\ell L_{\text{ab}}(\lambda)}{4\lambda^2}. \quad (21)$$

## 4 PMT rate

In this section we compare the PMT rates measured in deep seawater by the ANTARES [10] and NEMO [11] Collaborations with the calculations developed in Sects. 2 and 3.

The contribution of multi-photons coming from  $^{40}\text{K}$  decays to the rate of a PMT deployed in the deep sea has been calculated [12] and measured [11] and it turns out to be negligible. Thus, from (21), we can write the PMT rate as

$$\begin{aligned} R_{\text{th}} &= S_{\text{PMT}} \int_{\lambda_1}^{\lambda_2} d\lambda \Phi(\lambda) \text{QE}(\lambda) \epsilon(\lambda) \\ &= \text{Act}\ell S_{\text{PMT}} \int_{\lambda_1}^{\lambda_2} d\lambda \text{QE}(\lambda) \epsilon(\lambda) \frac{L_{\text{ab}}(\lambda)}{4\lambda^2}, \quad (22) \end{aligned}$$

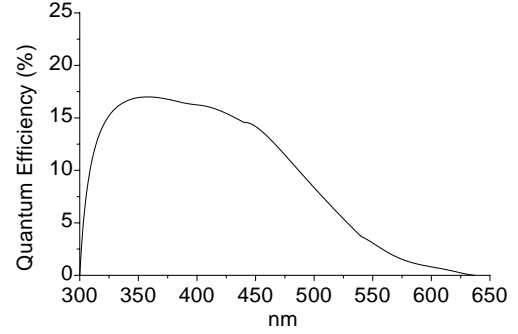


**Fig. 5.** Photocathode quantum efficiency of NEMO PMT versus photon wavelength

where  $\text{Act}$  and  $\ell$  are given in Sect. 3,  $S_{\text{PMT}}$  is the area of the PMT photocathode,  $\text{QE}$  the photocathode quantum efficiency,  $\epsilon$  the acceptance of the bathyscaphe input window and  $\lambda_1$  and  $\lambda_2$  the limits of sensitivity of the detector.

Several PMT deployments have been performed at different sites in the Mediterranean Sea south of Capo Passero (Sicily) by NEMO and south of Toulon and off Porto (Corsica) by ANTARES. In the NEMO tests of March and September 2000 at the site Lat.  $36^\circ \text{ N}$ , Long.  $16^\circ 03 \text{ E}$  (here called the KM3 NEMO site) a 2" EMI 9839A PMT, located in a stainless steel cylindrical container provided with a flat glass input window, was deployed at a depth of 2700 m. Figure 5 shows the quantum efficiency of the PMT bialkali photocathode calculated from the quoted 7.3 CB number [13]. The uniformity map of the photocathode is integrated with the geometrical acceptance and the light transmission of the glass input window in a Monte Carlo calculation. The resulting acceptance  $\epsilon(\lambda)$  is reported in Fig. 6. In Fig. 7 the inverse of the absorption (full points) and attenuation (open points) lengths measured at a depth of 2700 m in the KM3 NEMO site are reported [7]. The lines fitting the experimental data are obtained by scaling the pure water data [14]. Using these values of  $L_{\text{ab}}$  in (21) we obtain the expected photon flux  $\Phi(\lambda)$  shown in Fig. 8. From these  $\Phi(\lambda)$  values we can calculate by numerical integration the total flux between 300 and 600 nm for the KM3 NEMO site

$$502 \text{ photons cm}^{-2} \text{ s}^{-1}$$

and, from (22), the expected PMT rate

$$R_{\text{th}} = 387 \text{ Hz.}$$

This last result can be compared with the PMT rates measured at a depth of 2700 m at the KM3 NEMO site:

$$R_{\text{exp}} = (391.3 \pm 1.5(\text{stat.}) \pm 11.5(\text{sist.})) \text{ Hz.}$$

The ANTARES Collaboration deployed a HAMAMATSU 8" PMT located in a Benthos sphere and reported an upper limit on the contribution to the rate attributed to  $^{40}\text{K}$  decays of

$$R_{\text{exp}} < 20 \text{ kHz.}$$

With the values

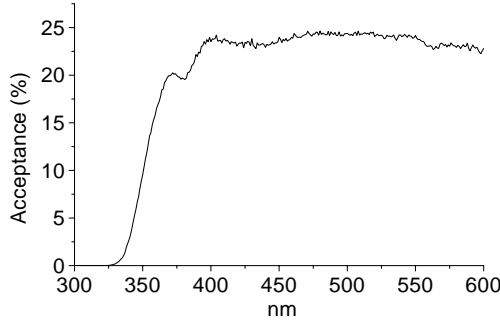


**Fig. 6.** Monte Carlo calculation of the NEMO PMT acceptance

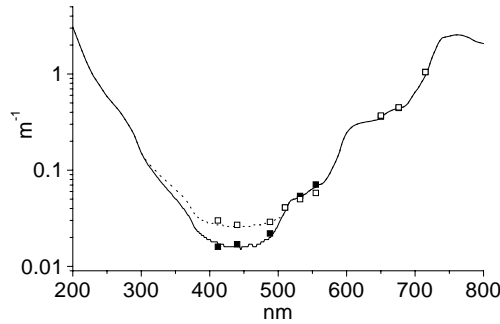


**Fig. 7.** Measured values of the inverse of the absorption (full points) and attenuation lengths (open points) in the KM3 NEMO site at a depth of 2700 m. The lines are obtained by scaling the pure water values

- (1) PMT area  $S_{\text{PMT}} = 280 \text{ cm}^2$  [10];
  - (2) water absorption lengths  $L_{\text{ab}}(\lambda)$  of the ANTARES site (Fig. 5.4.c of [15]);
  - (3) light transmission efficiency  $\epsilon(\lambda)$  of Fig. 9, calculated for an isotropic light flux from the Benthos sphere absorption lengths of Fig. 5.4.c of [15];
  - (4) photocathode quantum efficiency  $\text{QE}(\lambda)$  reported in Fig. 5.4.d of [15],
- Equation (21) gives the expected flux between 300 and 600 nm for the ANTARES site

$$403 \text{ photons cm}^{-2} \text{ s}^{-1},$$

and (22) the expected ANTARES PMT rate:

$$R_{\text{th}} = 18.1 \text{ kHz}.$$

These last results suffer from uncertainty regarding  $L_{\text{ab}}$  values, which are reported (in [15]) for the entire optical wavelength range on the basis of a single measurement made at 466 nm.

## 5 Direct and scattered photon flux

Following the procedure of Sect. 2.2, we can distinguish two contributions to the flux (7): the first one due to the direct photons, which do not make any collision before arriving on the surface  $dS$ , and the second one due to the photons experiencing some scattering [16].

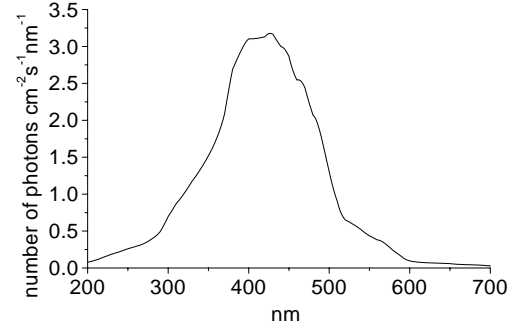


**Fig. 8.** Calculated photon flux at different wavelengths at a depth of 2700 m at the KM3 NEMO site

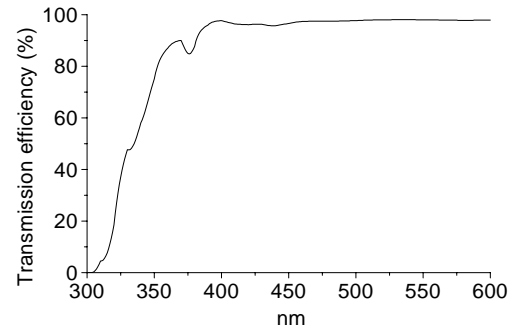


**Fig. 9.** Monte Carlo calculation of the ANTARES PMT acceptance

The flux of the direct photons can be obtained by putting in the second member of (17) the rate of the photons *generated* per unit volume ( $I_0$ ) in place of the photon *emitted* rate ( $I$ , see (15)), which contains the scattering contribution. We obtain, integrating over the whole space  $\tau$ ,

$$\frac{dN_{\text{dir}}}{dSdt} = I_0 \frac{L_{\text{at}}}{4}. \quad (23)$$

Ignoring the scattering contribution is equivalent to assuming this last value for the photon flux. In this case one underestimates the flux by a factor  $L_{\text{ab}}/L_{\text{at}}$  per each wavelength, as is evident from (7).

In analogy to (23), if we put in (17)

$$I_{\text{sc}} = I_0 \frac{L_{\text{ab}}}{L_{\text{sc}}}$$

(see (14)) in place of  $I$ , we obtain the flux of the scattered photons

$$\frac{dN_{\text{sc}}}{dSdt} = I_0 \frac{L_{\text{at}} L_{\text{ab}}}{4 L_{\text{sc}}}.$$

Substituting  $L_{\text{sc}}$  from (1) in the previous equation we have

$$\begin{aligned} \frac{dN_{\text{sc}}}{dSdt} &= I_0 \frac{L_{\text{at}}}{4} L_{\text{ab}} \left( \frac{1}{L_{\text{at}}} - \frac{1}{L_{\text{ab}}} \right) \\ &= I_0 \frac{L_{\text{ab}} - L_{\text{at}}}{4}, \end{aligned} \quad (24)$$

so that, from (7),

$$I_0 \frac{L_{\text{ab}}}{4} = \frac{dN}{dSdt} = \frac{dN_{\text{sc}}}{dSdt} + \frac{dN_{\text{dir}}}{dSdt}.$$

Considering now the wavelength dependence we have, from (20), (23) and (24)

$$\frac{dN_{\text{dir}}}{dSdt} = \text{Act}\ell \int_{\lambda_1}^{\lambda_2} d\lambda \frac{L_{\text{at}}(\lambda)}{4\lambda^2}, \quad (25)$$

$$\frac{dN_{\text{sc}}}{dSdt} = \text{Act}\ell \int_{\lambda_1}^{\lambda_2} d\lambda \frac{L_{\text{ab}}(\lambda) - L_{\text{at}}(\lambda)}{4\lambda^2} \quad (26)$$

as contributions of the direct and scattered light to the total flux, which in turn is, from (10)

$$\frac{dN}{dSdt} = \text{Act}\ell \int_{\lambda_1}^{\lambda_2} d\lambda \frac{L_{\text{ab}}(\lambda)}{4\lambda^2}.$$

From the absorption and attenuation length values of the KM3 NEMO site of Fig. 7 and from (25) and (26) it turns out that, out of  $502 \text{ photons cm}^{-2} \text{ s}^{-1}$  of the total flux, 362 are due to direct light and 140 to scattered light.

According to (25) and (26) we can write the PMT rates due to direct and scattered light as

$$R_{\text{dir}} = \text{Act}\ell S_{\text{PMT}} \int_{\lambda_1}^{\lambda_2} d\lambda \text{QE}(\lambda) \epsilon(\lambda) \frac{L_{\text{at}}(\lambda)}{4\lambda^2},$$

$$R_{\text{sc}} = \text{Act}\ell S_{\text{PMT}} \int_{\lambda_1}^{\lambda_2} d\lambda \text{QE}(\lambda) \epsilon(\lambda) \frac{L_{\text{ab}}(\lambda) - L_{\text{at}}(\lambda)}{4\lambda^2},$$

while the total rate  $R_{\text{th}}$  is given by (22). In the KM3 NEMO site, out of 387 Hz of the PMT rate, we would expect 261 Hz to be due to direct light and 126 Hz to scattered light.

*Acknowledgements.* I am indebted to D. Zanello for discussions, suggestions and critical reading of the manuscript.

## References

1. C.D. Mobley, Light and water (Academic Press, New York 1994) Chapt. 5.14
2. Frank.H. Attix, Introduction to radiological physics and radiation dosimetry (Wiley Interscience Pub., New York 1986) Chapt. 3.IX
3. M. Born, E. Wolf, Principles of optics (Pergamon Press, London, New York 1959) Chapt. 8.3.2
4. G. Neumann, W.J. Pierson, Principles of physical oceanography (Prentice-Hall, Englewood Cliffs, N.J. 1966) Chapt. 3
5. Tables of Radioisotopes  
<http://nucleardata.nuclear.lu.se/nucleardata/toi>
6. G. Cognetti, M.Sarà, G. Maguzzu, Biologia Marina (Calderini Edt., Bologna 1999) Chapt. 3
7. A. Capone et al., Proceedings 26th ICRC HE.6.3.05 **2** (Salt Lake City, 1999) p. 444
8. P. Guibot Atlas hydrologique de la mediterranean (IFREMER-SHOM, France 1987) p. 131–132
9. ICRU Report 37 Stopping Power for Electrons and Positrons (International Commission on Radiation Units and Measurements, Bethesda, MD. 1984) p. 208–209
10. P. Amram et al., Astroparticle Physics **13**, 127 (2000)
11. F. Ameli, M. Bonori, A. Capone, F. Massa, R. Masullo, M. Petrucetti, The  $^{40}\text{K}$  station: a single photon detector of the optical background in deep sea, to be published; F. Ameli, M. Bonori, A. Capone, F. Massa, Measurement of optical background in the site for NEMO km<sup>3</sup> undersea neutrino telescope, to be published
12. C.H. Wiebush, PITHA 95/37 (1955)
13. THORN EMI: Photomultipliers
14. R.C. Smith, K.S. Baker, Applied Optics **20**, 177 (1981)
15. ANTARES proposal <http://antares.in2p3.fr>
16. R.D. Evans, The atomic nucleus (McGraw-Hill book comp., New York 1955) Chapt. 25.4